Mixed Convection Heat Transfer over a Porous Elastic Sheet with Temperature-Dependent Transport Properties.

HANUMESH VAIDYA
Department of Mathematics, SSA Government First Grade College (Autonomous),
Ballari-583 101, Karnataka, India.
Email: hanumeshvaidya@gmail.com

Abstract:
The present article examines the mixed convection and heat transfer in a viscous fluid flow towards the nonlinear stretching porous sheet of variable thickness. The nonlinear governing equations with suitable boundary conditions are initially cast into dimensionless form by similarity transformations and are then solved via the Keller-box method. A limited parametric study is undertaken to determine the sensitivity and changes in the flow and temperature fields with respect to variations in the buoyancy parameter, the temperature dependent viscosity and thermal conductivity parameters, the surface velocity power index, and the Prandtl number which are presented in graphical and tabulated formats. The analysis reveals interesting flow and heat transfer characteristics for increasing values of the wall thickness, porous parameter and buoyancy parameters.

Keywords: Permeability; Keller-box method; flow and heat transfer, Variable thickness.

1.Introduction

The investigation of two-dimensional boundary layer flow over a stretching sheet has produced much interest over the years due to its various modern applications, for example, aerodynamic extrusion of polymer sheets, continuous stretching, rolling and manufacturing plastic films and artificial fibers. Boundary layer flow happens on moving persistent surfaces such as those of long thread between a feed roll and a wind-up roll. The pioneering work of Sakiadis [1-2] has made a revolution in the field of flow through moving surface and is the first among others to discuss such flow behaviours theoretically and that is followed by the work of Crane [3] and the test confirmation work of Tsou et al. [4]. There are several extensions of this problem considering different geometry (Prasad et al. [5-6]). In addition to this, there are many practical situations/ conditions are used to control the flow field. In many practical situations, the resulting flow and the thermal field are determined by surface motion and thermal buoyancy. It is well known that the buoyancy force stemming from the heating or cooling of a continuous stretching sheet alters the flow and the thermal fields and thereby the heat transfer characteristics in manufacturing processes. However, the significance and impact of the buoyancy force were not assessed in the studies reviewed above. Furthermore, the study of convection heat transfer around or past a sphere, a cone, and a wedge has practical applications. The flow of heat around these objects has applications in fields that include spacecraft design and nuclear reactors, Ostrach [7] studied free-convection flow about a flat plate and obtained theoretical and experimental results for velocity and temperature distributions. Mixed convection heat transfer at a stretching sheet with variable temperature was investigated by Vajravelu [8]. Ishak et al. [9] analyzed the hydromagnetic effects to mixed convection flow near a vertical stretching sheet.

Reestablished enthusiasm for the stretching sheet problem was started by a realization that some physical problems may be better modeled by a nonlinearly stretching sheet. Some physical situations occur in which a nonlinearly stretching sheet is a better model. With several industrial applications in mind, Lee 10] introduced the idea of variable thickness in theoretical studies. Fang et al. [11] studied the behaviour of boundary layer flow over a stretching sheet with variable thickness and considered a special type of non-

linear stretching $u_w(x) = U_0(x+b)^m$ for different values of *m* where *b* and *Uo* are constants. Khader et al. [12] continued the work of Fang et al. [11] and obtained the numerical solution for the slip velocity effect. Recently, Prasad et al. [13], Vajravelu et al. [14] and Prasad et al. [15], focused on heat transfer characteristics of fluid flow over a stretching sheet with variable thickness and power-law velocity in the presence of a variable magnetic field.

Most of the studies above restricted their analysis to the flow and heat transfer over a horizontal or a vertical plate and assumed the thermo-physical properties of the ambient fluid to be constant. However, it is evident that these physical properties may change with temperature, especially the fluid viscosity and fluid thermal conductivity (Prasad et al. [16], Vajravelu et al. [17], Prasad et al. [18] and Hassanien [19]). For lubricating fluids, heat generated by internal friction and the corresponding rise in the temperature affects the physical properties of the fluid, and the properties of the fluid can no longer be assumed to be constant. The increase in temperature leads to an increase in the transport processes including heat transfer at the wall. Therefore, to predict the flow and heat transfer rates, it is necessary to take into account the variable fluid properties. From the literature, we find no evidence of previous studies on the combined effects of variable fluid properties and mixed convection in flow over a slender stretching sheet with variable thickness.

The problem studied here is the mixed convection flow over a porous stretching sheet with variable thickness. The thermo-physical properties of the fluid are taken into account. The coupled non-linear partial differential equations modeling the flow problem have been transformed to a system of coupled non-linear ordinary differential equations. These equations have been solved numerically using the Keller-box method, which is essentially a second-order finite difference method. Computed numerical results for the flow and heat transfer characteristics are found to be in good agreement with experimental results in the literature. The results show that the fluid flow is significantly influenced by various fluid parameters. It is expected that the results obtained will not only provide useful information for industrial applications but would also serve to complement and validate previous works.

2.Mathematical formulation

Consider a mixed convection boundary layer flow of a viscous incompressible fluid in the presence past a permeable stretching vertical heated sheet with variable thickness. The origin is located at the slit, through which the sheet is drawn in the fluid. Two equal and opposite forces are applied impulsively along the *x*-axis so that the sheet is stretched, keeping the origin fixed. The stationary coordinate system has its origin located at the center of the sheet with the x-axis extending along the sheet, while the y-axis is measured normal to the surface of the sheet and is positive in the direction of the sheet to the fluid. We assume that the wall is permeable and that the sheet is stretched with a velocity $U_w(x) = U_0(x+b)^m$ where U_0 is constant, *b* is a physical parameter related to stretching sheet and *m* is the velocity exponent parameter. The sheet is not flat and its thickness is defined by $y = \mathrm{A}(x+b)^{(1-m)/2}$, where the coefficient A is small so that the sheet is sufficiently thin, to avoid pressure gradient along the sheet $(\partial p/\partial x = 0)$. For different applications, due to the acceleration or deceleration of the sheet, the thickness of the stretched sheet may decrease or increase with distance from the slot, which is dependent on the value of the velocity power index *m*. Under these assumptions and invoking the Boussinesq and boundary layer approximations, the governing equations for mass, momentum and energy for the model in the presence of temperature dependent fluid properties are

$$\frac{\partial u}{\partial x} + \frac{\partial u}{\partial y} = 0, \tag{1}$$

$$\rho_\infty\left(u\frac{\partial u}{\partial x} + \mathrm{v}\frac{\partial u}{\partial y}\right) = \frac{\partial}{\partial y}\left(\mu\frac{\partial u}{\partial y}\right) \pm g\beta(T - T_\infty) - \frac{\mu}{K'}u, \tag{2}$$

$$\rho_\infty c_p\left(u\frac{\partial T}{\partial x} + \mathrm{v}\frac{\partial T}{\partial y}\right) = \frac{\partial}{\partial y}\left(k(T)\frac{\partial T}{\partial y}\right), \tag{3}$$

where u and v are the fluid velocity components in the streamwise and cross-stream directions, respectively. The suffix denotes partial differentiation with respect to the independent variables, ρ_∞ is the constant fluid density, g is the acceleration due to gravity, β is the coefficient of thermal expansion, μ is the coefficient of viscosity which varies as an inverse function of temperature and is as follows

$$\mu = \frac{\mu_\infty}{\left[1+\gamma\left(T-T_\infty\right)\right]} \quad \text{i.e.,} \quad \frac{1}{\mu} = a\left(T-T_r\right), \tag{4}$$

where, $a = \dfrac{\gamma}{\mu_\infty}$ and $T_r = T_\infty - \dfrac{1}{\gamma}$.

Here both a and T_r are constants, T is the temperature; T_∞ and μ_∞ are the constant ambient temperature and coefficient of viscosity respectively far from the sheet. The stretching vertical heated porous sheet with the upper half of the flow field being assisted and the lower half of the flow field being opposed by the buoyancy force. For the assisting flow, the x-axis points upwards in the direction of the stretching hot surface such that the stretching induced flow and the thermal buoyant flow assist each other. For the opposing flow, the x-axis points vertically downwards in the direction of the stretching hot surface but in this case, the stretching induced flow and the thermal buoyant flow oppose each other. The reverse trend occurs if the sheet is cooled below the ambient temperature. C_p is the specific heat at constant pressure and $k(T)$ is the temperature-dependent thermal conductivity. We consider the temperature-dependent thermal conductivity in the form (see Vajravelu et al. [15] and Prasad et al. [16])

$$k(T) = k_\infty\left(1+\frac{\varepsilon}{\Delta T}\left(T-T_\infty\right)\right) \tag{5}$$

where $\Delta T = T_w - T_\infty = \dfrac{C}{l}\left(x+b\right)^r$, T_w is the sheet temperature, C is a constant, l is the characteristic length, ε is the thermal conductivity parameter and k_∞ is thermal conductivity of the fluid away from the sheet, r is a wall temperature parameter.

The appropriate boundary conditions for the problem are

$$\begin{aligned} &u\left(x,y\right)=U_w=U_0\left(x+b\right)^m, \mathrm{v}\left(x,y\right)=0, T\left(x,y\right)=T_w=\frac{C}{l}\left(x+b\right)^r \ at \ \ y=A\left(x+b\right)^{\frac{1-m}{2}}, \\ &u\left(x,y\right)\to 0, \qquad T\left(x,y\right)\to T_\infty \ \ as \ \ y\to\infty. \end{aligned} \tag{6}$$

It should be noted that a positive m indicates stretching and a negative value indicates a shrinking sheet. Now we transform the system of Eqs. (1) - (3) into a dimensionless form. To this end, let the dimensionless similarity variable be

$$\eta = y\sqrt{\frac{m+1}{2}\frac{U_0}{\nu_\infty}}\,(x+b)^{\frac{m-1}{2}}, \tag{7}$$

the stream function $\psi(x,y)$ and the dimensionless temperature distribution $\theta(\eta)$ be

$$\psi(x,y) = f(\eta)\sqrt{\frac{2}{m+1}U_0\nu_\infty}\,\left(x+b\right)^{\frac{m+1}{2}}, \ \theta\left(\eta\right) = \frac{\left(T-T_\infty\right)}{\left(T_w-T_\infty\right)}. \tag{8}$$

Using (8) the velocity components can be written as

$$u = U_w f'(\eta) \ \text{ and } \ \mathrm{v} = -\sqrt{\nu_\infty\frac{m+1}{2}U_0}\,(x+b)^{\frac{m-1}{2}}\left[f(\eta)+\eta f'(\eta)\left(\frac{m-1}{m+1}\right)\right], \tag{9}$$

Here the prime denotes differentiation with respect to η. In the present work, it is assumed $m>-1$ for the validity of the similarity variable. Using equations (7) - (9), Eqs. (2), (3) and (6) now reduce to

$$\left(\frac{f''}{\left(1-\theta/\theta_r\right)}\right)' + ff'' - \frac{2m}{(m+1)}f'^2 - K_1 f' + \lambda\theta = 0, \tag{10}$$

$$\left[(1+\varepsilon\theta)\theta'\right]' + \Pr\left(f\theta' - \frac{2r}{m+1}\theta f' \right) = 0, \tag{11}$$

The non-dimensional parameters θ_r, K_1, λ *and* Pr are respectively, denote the fluid viscosity parameter, porous parameter, buoyancy or mixed convection parameter, the Prandtl number and are defined as follows $\theta_r = \frac{T_r - T_\infty}{T_w - T_\infty} = -\frac{1}{\gamma\left(T_w - T_\infty\right)}$, $K_1 = \nu_\infty / K'b$, $\lambda = \frac{\pm g\beta C}{l U_0^2}$ and $\Pr = \frac{\nu_\infty}{\alpha_\infty}$.

The mixed convection parameter λ is independent of x if $r = 2m-1$. Thus, the similarity solutions are obtained under this limitation when $\lambda \neq 0$. We note that when $r = 2m-1$, λ is a constant, with $\lambda > 0$ and $\lambda < 0$ corresponding to assisting flow and opposing flow, respectively, while $\lambda = 0$ $\left(i.e., T_w = T_\infty\right)$ represents the case when the buoyancy force is absent (that is, pure forced convection flow). On another hand, if λ is of a significantly greater order of magnitude than unity, the buoyancy forces will be dominant and the flow will essentially be free convective. Hence, combined convective flow exists when $\lambda = O(1)$. Under the limitation $r = 2m-1$, Eq. (11) becomes

$$\left[(1+\varepsilon\theta)\theta'\right]' + \Pr\left(f\theta' - \frac{2(2m-1)}{m+1}\theta f' \right) = 0, \tag{12}$$

and the corresponding boundary conditions are $(m \neq 1)$

$$\left.\begin{aligned} &f(\alpha) = \alpha\frac{1-m}{1+m},\ f'(\alpha) = 1, \theta(\alpha) = 1, \\ &\theta(\infty) = 0,\ f'(\infty) = 0. \end{aligned}\right\} \tag{13}$$

The value of θ_r is determined by the viscosity of the fluid and the operating temperature difference. If θ_r is large then $(T_\infty - T_w)$ is small and the effects of variable viscosity can be neglected. On another hand, for smaller values of θ_r, the fluid viscosity changes markedly with temperature. That is, the variable viscosity becomes very important. Also, bearing in mind that the liquid viscosity varies differently with temperature compared to a gas, it is important to note that θ_r is negative for liquids and positive for gasses. Further, the viscosity of a fluid usually decreases with an increase in the temperature. Here $\alpha = A\sqrt{\frac{m+1}{2}\frac{U_0}{\nu_\infty}}$ is the wall thickness parameter and $\eta = \alpha = A\sqrt{\frac{m+1}{2}\frac{U_0}{\nu_\infty}}$ indicates the plate surface. In order to facilitate simulations, we define $f(\xi) = f(\eta - \alpha) = f(\eta)$ and $\theta(\xi) = \theta(\eta - \alpha) = \theta(\eta)$.

The similarity equations become

$$\left(\frac{f''}{(1-\theta/\theta_r)}\right)' + ff'' - \frac{2m}{(m+1)} f'^2 - K_1 f' + \lambda\theta = 0, \tag{14}$$

$$\left[(1+\varepsilon\theta)\theta'\right]' + \Pr\left(f\theta' - \frac{2(2m-1)}{m+1}\theta f' \right) = 0, \tag{15}$$

and the corresponding boundary conditions are $(m \neq 1)$

$$\begin{aligned} &f(0) = \alpha\frac{1-m}{1+m},\ f'(0) = 1\ , \theta(0) = 1, \\ &\theta(\infty) = 0,\ f'(\infty) = 0. \end{aligned} \tag{16}$$

where the prime denotes the differentiation with respect to ξ . Based on the variable transformation, the solution domain is fixed from 0 to ∞. The shear stress and wall temperature gradient respectively become $f''(\alpha)=f''(0)$ and $\theta'(\alpha)=\theta'(0)$.

For practical purposes, the important physical quantities of interest are the local skin friction C_{fx} and the local Nusselt number Nu_x defined as;

$$C_{f_x} = \frac{2\nu_\infty \left(u_y\right)_{y=A(x+b)^{\frac{1-m}{2}}}}{U_w^2} = 2\sqrt{(m+1)/2}\,\left(\mathrm{Re}_x\right)^{-1/2} f''(0),$$
$$Nu_x = \frac{(x+b)\left(T_y\right)_{y=A(x+b)^{\frac{1-m}{2}}}}{\left(T_w - T_\infty\right)} = -\sqrt{(m+1)/2}\,\left(\mathrm{Re}_x\right)^{1/2}\theta'(0), \tag{17}$$

where $\mathrm{Re}_x = \dfrac{U_w(x+b)}{\nu_\infty}$ is the local Reynolds number.

3.Results and discussion

Equations (14) and (15) are highly non-linear, coupled ordinary differential equations are solved with boundary condition (16) via Keller-box method (See Vajravelu and Prasad [19]). The numerical solutions are obtained in four steps and for numerical calculations, a uniform step size of $\Delta\xi = 0.01$ is found to be satisfactory and the solutions are obtained with an error tolerance of 10^{-6} in all the cases. In order to validate the method used in this study and to judge the accuracy of the results, the skin friction and the wall temperature gradient are compared with the previously published results of Fang et al. [11], Khader and Megahed [12] for several special cases in which some thermo physical fluid properties are neglected. The results are found to be in excellent agreement and are shown in Table I. In order to get a clear insight of the physical problem numerical results are obtained for different values of pertinent parameters such as the fluid viscosity parameter θ_r, the mixed convection parameter λ, the thermal conductivity parameter ε, the velocity power index parameter *m*, and the Prandtl number Pr. Analytical solutions have been obtained for the special case when $\theta_r \to \infty$, m = 1, $\lambda = 0$, and $K_1 = 0$. We present the numerical results graphically for the horizontal velocity profile f' with ξ and the temperature profile θ with ξ for different parameter values in Figs. 1-2. We observe that both f' and θ decrease asymptotically to zero with the distance from the boundary. The computed numerical values for the skin friction $f''(0)$ and the wall temperature gradient $\theta'(0)$ are given in Table 2.

Figures 1(a)–1(b) give a qualitative representation of the horizontal velocity f' for increasing values of α. Fig 1(a) depicts the effect of λ on f'. The presence of thermal buoyancy effects is indicated by a finite value of λ $(\lambda \neq 0)$. It is observed that an increase in the value of λ leads to an increase in f'. Physically $\lambda > 0$ implies heating of the fluid or cooling of the surface, $\lambda < 0$ suggests cooling of the fluid or heating of the surface, and $\lambda = 0$ corresponds to the absence of the mixed convection. An increase in λ means an increase in the temperature difference $(T_w - T_\infty)$ which leads to an enhancement in f' due to the enhanced convection, and thus an increase in the momentum boundary layer thickness. Fig.1 (b) represents the effect of increasing θ_r on the velocity f'. The velocity decreases with increasing θ_r and as $\theta_r \to 0$ the momentum boundary layer thickness decreases. The velocity distribution is linear in shape for higher values of α. This is due to the fact that for a given fluid, when θ_r is smaller, higher is the temperature difference between the wall and the ambient fluid. The results clearly demonstrates that θ_r is the indicator of the variable fluid viscosity with temperature which has a substantial effect on the velocity component f' and hence on the skin friction. The effect of α on f' for zero and non zero values of *m* is demonstrated in Fig.1(c). It shows that the velocity profile decreases with an increase in the value of α , this shows that the momentum boundary layer thickness becomes thinner as α increases. This phenomenon is even true for

zero and negative value of *m*. The effect of *m* is to enhance the velocity profile which in turn increases the boundary layer thickness. Fig. 1(d) explains the effect of α on f' for different values of K_1. It is obvious that the presence of a porosity presents a higher constraint to the fluid flow, which reduces the fluid velocity and hence induces an increase in the absolute value of the velocity gradient at the surface.

In Figs. 2(a)–2(e) the numerical results for the temperature distribution θ for several sets of values of the governing parameters are presented. Fig 2(a) illustrates the effect of λ on θ for increasing values of α. With the increase in λ, temperature field is suppressed and consequently thermal boundary layer thickness becomes thinner and as a result rate of heat transfer from the plate increases, this is due to buoyancy force. Fig 2(b) elucidates the effect of θ_r on θ for different values of α. From the graphical representation, we see that the effect of increasing value of θ_r is to enhance the temperature. This is because of the fact that an increase in θ_r results in an increase in the thermal boundary layer thickness. Fig 2(c) exhibits the nature of temperature field for the variation of α for different values of *m*. Increase in α is to reduce the temperature distribution and thermal boundary layer becomes thinner for higher values of α. Fig 2(d) exhibits the effect of α on θ for increasing values of K_1. As α increases, the temperature profile increases. This can be observed even for the increasing values of K_1. As explained above, the porous parameter gives rise to a resistive force to fluid thus increases the fluid temperature. The effect of Pr on θ is exhibited in Fig 2(e) for zero and nonzero values of ε. Temperature is found to decrease with increasing Pr. An increase in the Pr reduces the thermal boundary layer thickness. Pr signifies the ratio of momentum diffusivity to thermal diffusivity. Fluids with lower Pr possess higher thermal conductivities and thicker thermal boundary layer structures so that heat can diffuse from the wall faster than higher Pr fluids thinner boundary layers. Hence, Pr can control the rate of cooling in conducting flows. Further, it is quite evident from the graph that the fluid temperature is found to increase with increasing values of ε which leads to a fall in the rate of heat transfer from the flow to the surface. This is due to the fact that the assumption of temperature-dependent thermal conductivity suggests the reduction in the magnitude of the transverse velocity by a quantity $\partial k(T)/\partial y$. Therefore, the rate of cooling is much faster for the coolant material having small thermal conductivity parameter.

The effects of the physical parameters on the skin friction $f''(0)$ and the wall-temperature gradient $\theta'(0)$ are tabulated in Table II. It is observed that for increasing values of λ there is an increase in $f''(0)$ whereas a decrease in $\theta'(0)$ and exactly opposite in the case of θ_r. It is also noticed that the effect of *m* is to decrease in both $f''(0)$ and $\theta'(0)$. Increasing Pr decreases $\theta'(0)$ and is reverse for increasing values of. Further, it is interesting to notice that for shrinking sheet case ($m < 1$) there is a decrease in both $f''(0)$ and $\theta'(0)$ for increasing values of α, whereas an opposite trend is observed for stretching sheet case ($m > 1$).

4.Conclusion

In this study, we sought to understand the effect of variable thickness on a stretching surface. Some of the interesting findings of the study are summarized below.

- The effect of the porous parameter is to reduce the fluid velocity and to increase the temperature field.
- The rate of heat transfer increases with increasing porous parameter and the Prandtl numbers.
- The effect of the variable thermal conductivity parameter is to enhance the temperature field.
- The effect of increasing the mixed convection parameter is to increase the momentum boundary layer thickness whereas to decreases the thermal boundary layer thickness.
- The dimensionless velocity distribution at a point near the plate decreases as the wall thickness parameter increases and hence the thickness of the boundary layer becomes thinner when $m < 1$.
- The effect of Prandtl number is to decrease the thermal boundary layer thickness and the wall-temperature gradient.

References

[1]. Sakiadis, B.C. “Boundary layer behaviour on continuous solid surfaces", Amer. Inst. Chem. Engng. J., (1961a), Vol. 7, p. 26.

[2]. Sakiadis, B.C. ``Boundary layer behaviour on continuous solid flat surfaces", Amer. Inst. Chem. Engng. J. (1961b), Vol. 7, p. 221.

[3]. Crane, L.J. (1970), ``Flow past a stretching sheet", Z.A.M.P., Vol. 21, p. 645.

[4]. Tsou, F.K., Sparrow, E.M. and Goldstein, R.J. ``Flow and heat transfer in the boundary layer on a continuous moving surfaces", Amer Inst. Chem. Engng. J., (1961), Vol. 7, p. 467.

[5]. K.V. Prasad, M. Subhas Abel, Sujit Kumar Khan, "Momentum and heat transfer in visco-elastic fluid flow in a porous medium over a non-isothermal stretching sheet", International Journal of Numerical Methods for Heat & Fluid Flow, (2000) Vol. 10(8), pp.786-801.

[6]. K.V. Prasad, M. Subhas Abel, Ambuja Joshi, Oscillatory Motion of a Viscoelastic Fluid over a Stretching Sheet in Porous Media, (2000) Vol.3(1),pp. 61-68.

[7]. S. Ostrach, An analysis of laminar free convection flow and heat transfer about a flat plate parallel to the direction of generating body force, NACA Tech. Note 1111 (1953).

[8]. K. Vajravelu, Convection heat transfer at a stretching sheet with suction or blowing, J. Math. Anal. Appl. 188 (1994) 1002–1011.

[9]. Ishak, R. Nazar and I. Pop: Hydromagnetic flow and heat transfer adjacent to a stretching vertical sheet, Heat Mass Transfer. 44 (2008) 921–927.

[10]. L.L. Lee, Boundary layer over a thin needle, Phys.of Fluids.10 (1967)822- 828.

[11]. T Fang, J Zhang, Y Zhong, Boundary layer flow over a stretching sheet with variable thickness, Appl. Math. Comput. 218 (2012)7241-7252.

[12]. M. M. Khader, A.M. Megahed. Boundary Layer Flow Due to a Stretching Sheet with a Variable Thickness and Slip Velocity, Journal of Applied Mechanics and Technical Physics, Vol. 56,(2), pp. 241–247(2015).

[13]. K.V Prasad, K. Vajravelu, Hanumesh Vaidya, MHD casson nanofluid flow and heat transfer at a stretching sheet with variable thickness. J. Nanofluids. **5**, 1–13 (2016).

[14]. K Vajravelu, KV Prasad, Chiu-On Ng, Hanumesh Vaidya, MHD Flow and Heat Transfer Over a Slender Elastic Permeable Sheet in a Rotating Fluid with Hall Current, Int. J. Appl. Comput. Math (2016). doi:10.1007/s40819-016-0291-3.

[15]. K.V. Prasad, K. Vajravelu, Hanumesh Vaidya, Robert A. Van Gorder, MHD flow and heat transfer in a nanofluid over a slender elastic sheet with variable thickness, Results in Physics 7 (2017) 1462–1474.

[16]. K. Vajravelu, , K V Prasad, Hanumesh Vaidya, Influence of hall current on MHD flow and heat transfer over a slender stretching sheet in the presence of variable fluid properties. Commun. Num. Anal. **1**, 17–36 (2016).

[17]. K.V Prasad, H. Vaidya, K. Vajravelu and M.M. Rashidi, ‘Effects of Variable Fluid Properties on MHD Flow and Heat Transfer over a Stretching Sheet with Variable Thickness’, Journal of Mechanics, (2016) pp. 1–12. doi: 10.1017/jmech.2016.101.

[18]. I.A. Hassanien, The effect of variable viscosity on flow and heat transfer on a continuous stretching surface, ZAMM. 77 (1997) 876–880.

[19]. K. Vajravelu and K.V. Prasad, Keller-box method and its application, HEP and Walter De Gruyter GmbH, Berlin/Boston (2014).

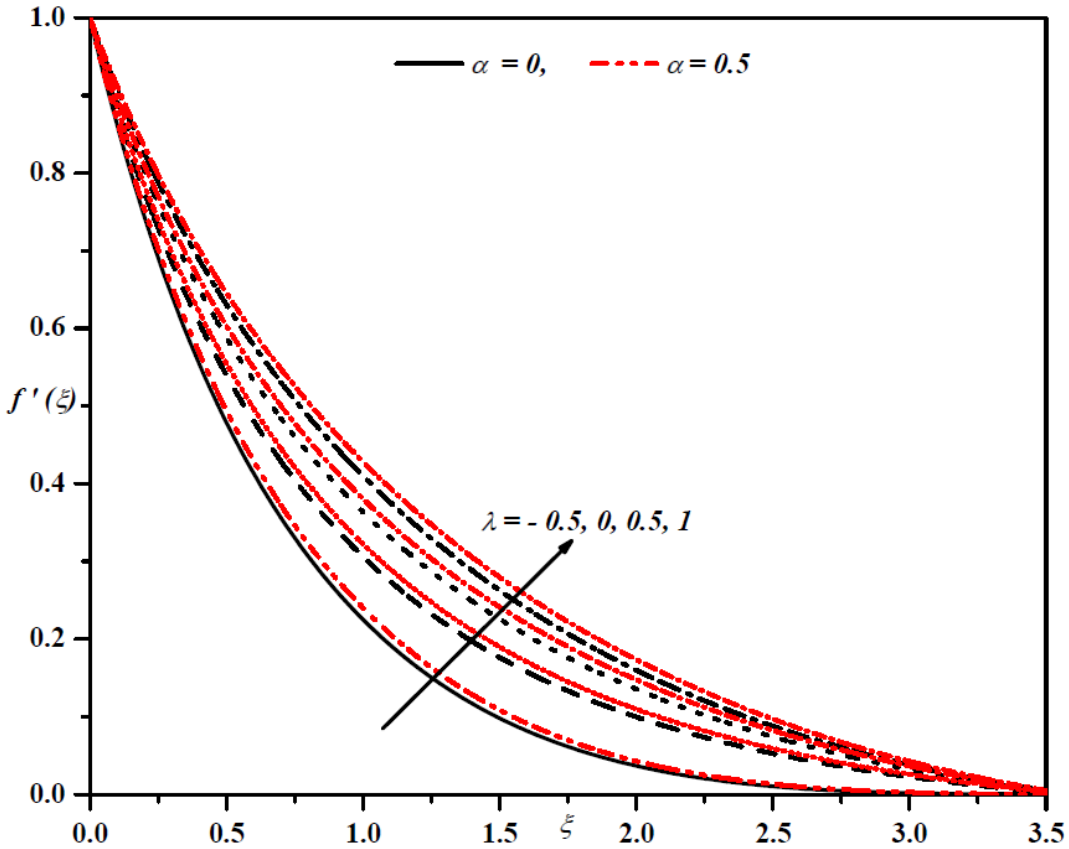

Fig.1(a): Horizontal velocity profiles for different values of λ and α with $Pr = 1$, $\varepsilon = 0.1$, $K_1 = 0.1$, $m = 2.0$, $\theta_r = -5.0$.

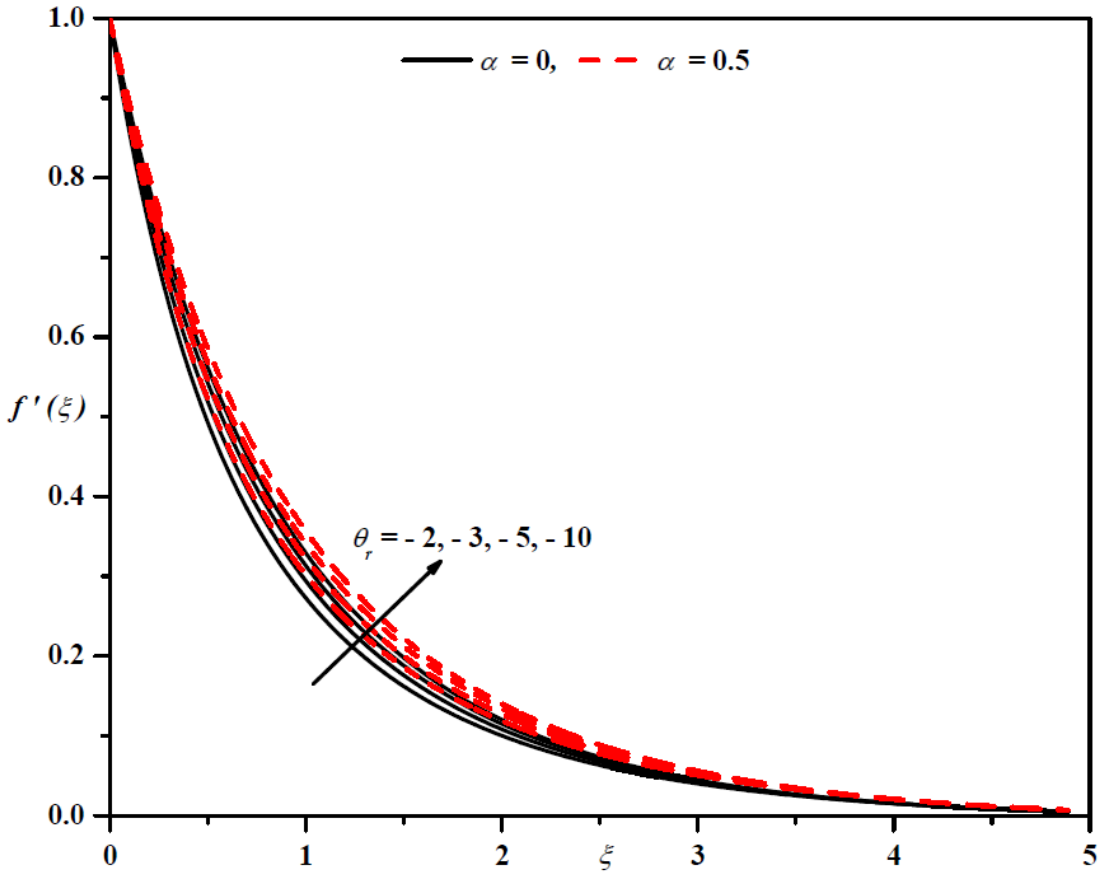

Fig.1(b): Horizontal velocity profiles for different values of θ_r and α with $\lambda = 0.1$, $Pr = 1$, $K_1 = 0.1$, $m = 2$, $\varepsilon = 0.1$.

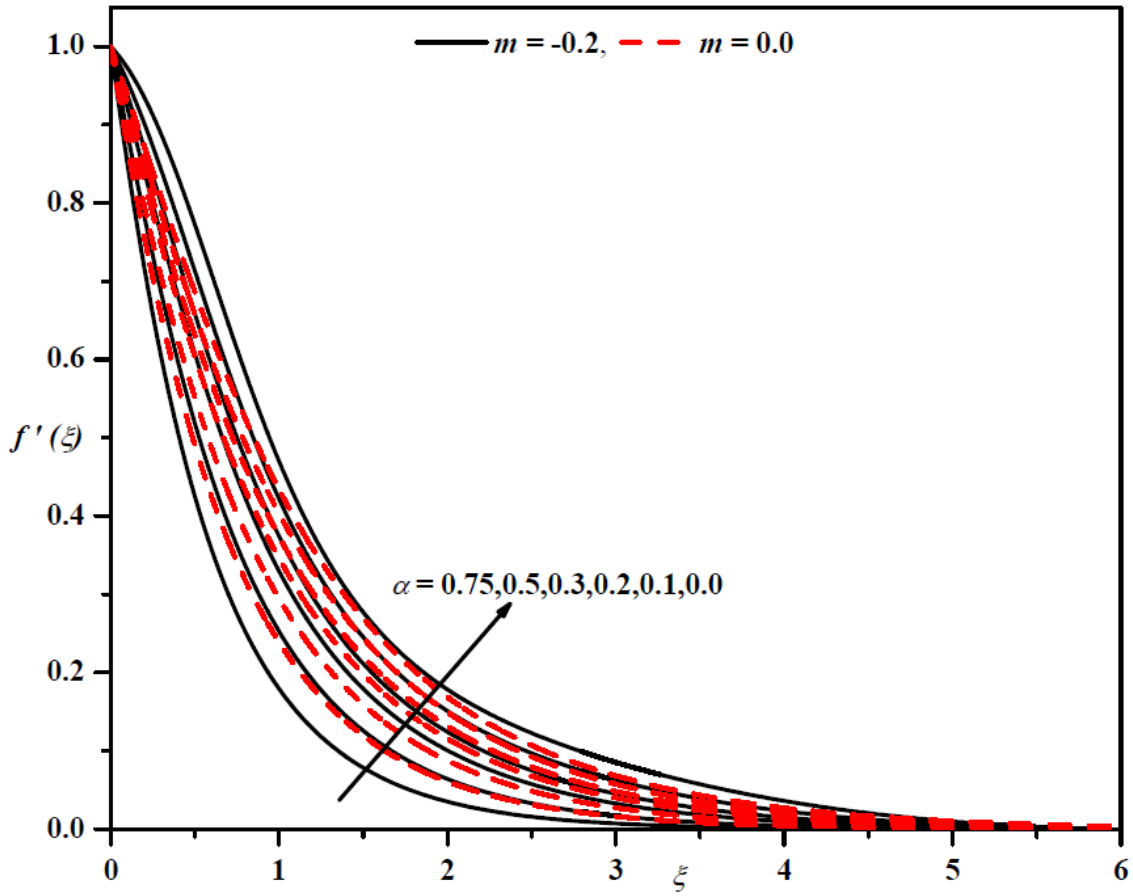

Fig.1(c): Horizontal velocity profiles for different values of α and m with $Pr = 1.0$, $\varepsilon = 0.1$, $K_1 = 0.0$, $\theta_r = -5.0$, $\lambda = 0.1$

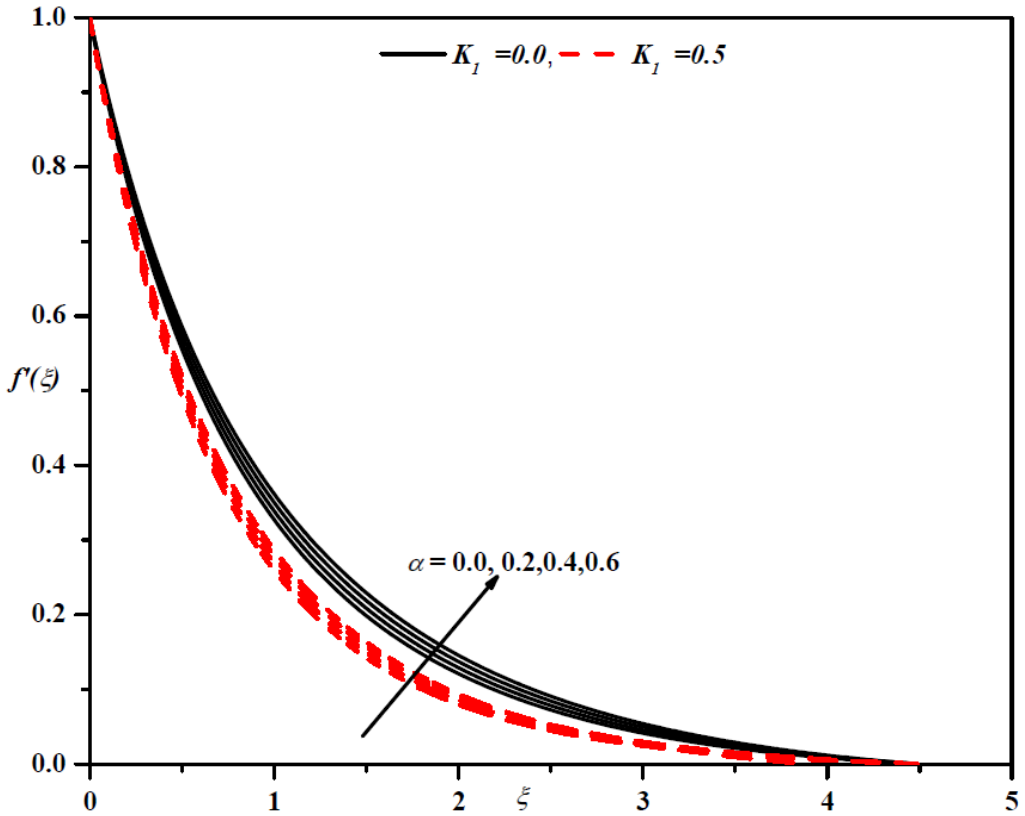

Fig.1(d): Horizontal velocity profiles for different values of α and K_1 with $\theta_r = -5.0$, $\lambda = 0.1$, $\varepsilon = 0.1$, $m = 2.0$.

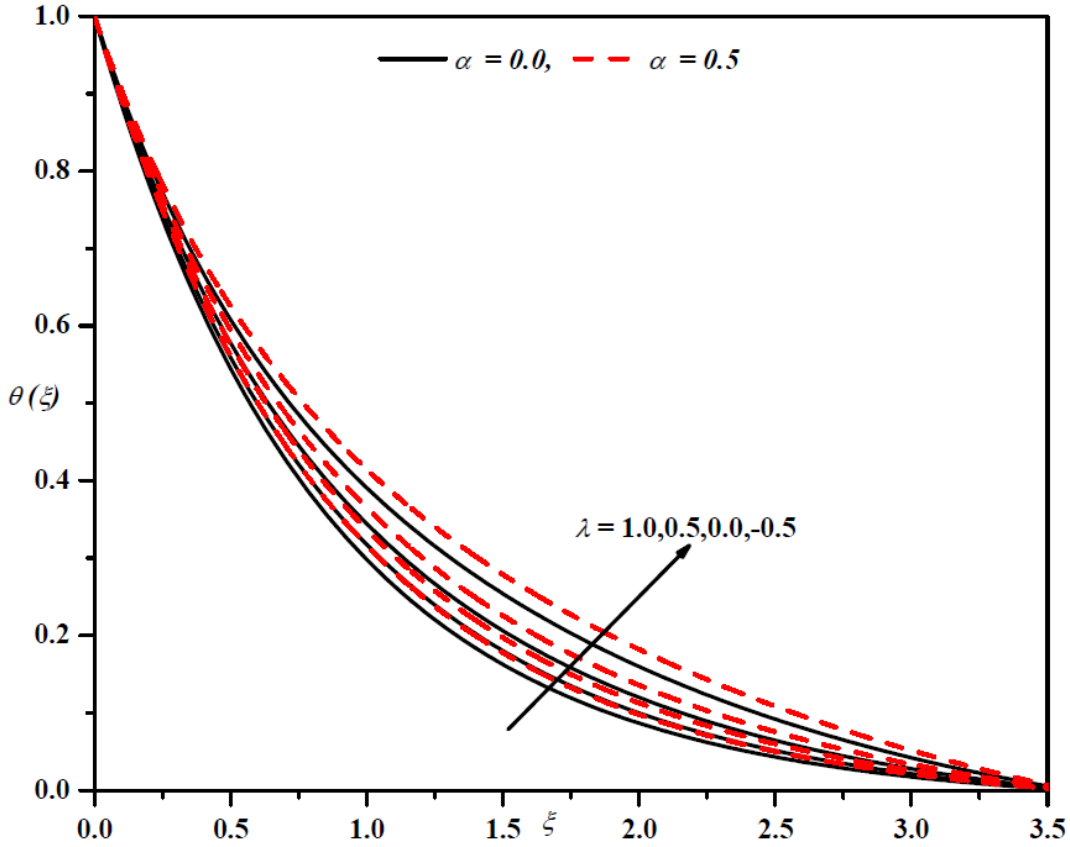

Fig.2(a): Tempearture profiles for different values of λ and α when $Pr = 1.0$,

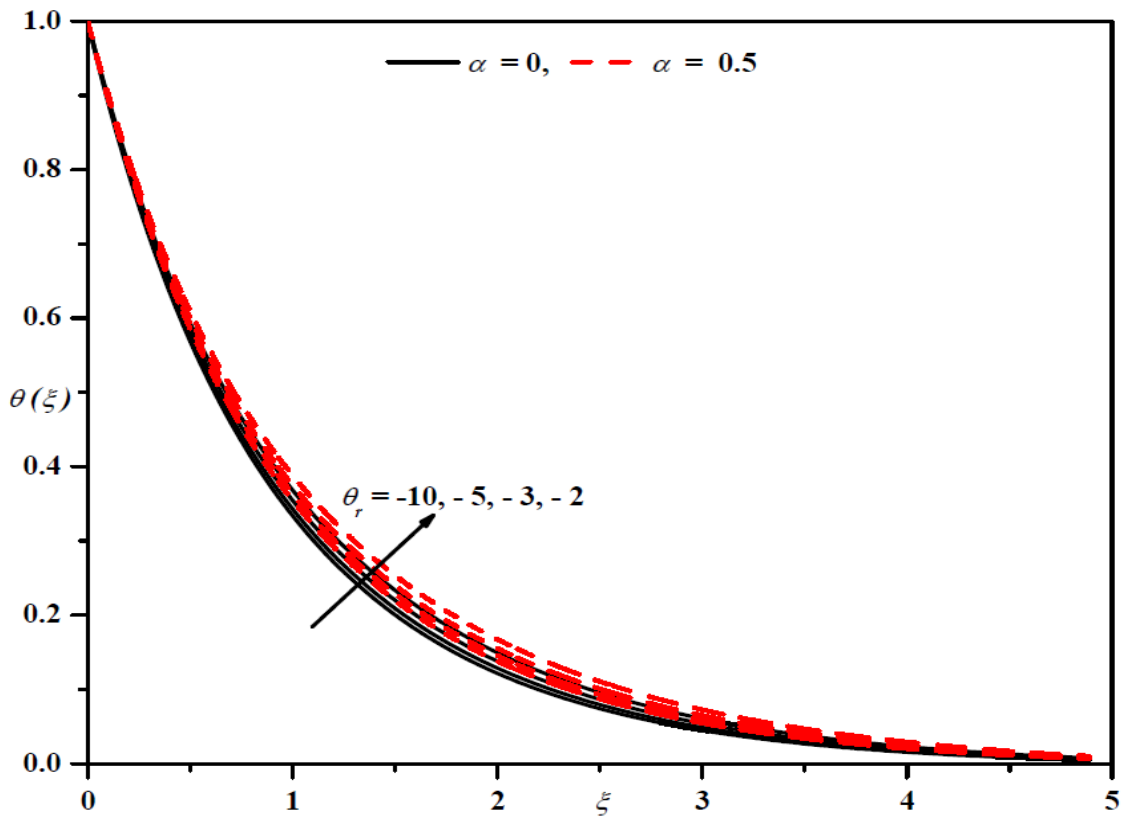

Fig.2(b): Temperature profiles for different values of θ_r and α with $\lambda = 0.1$, $K_r = 0.1$, $m = 2$, $\varepsilon = 0.1$.

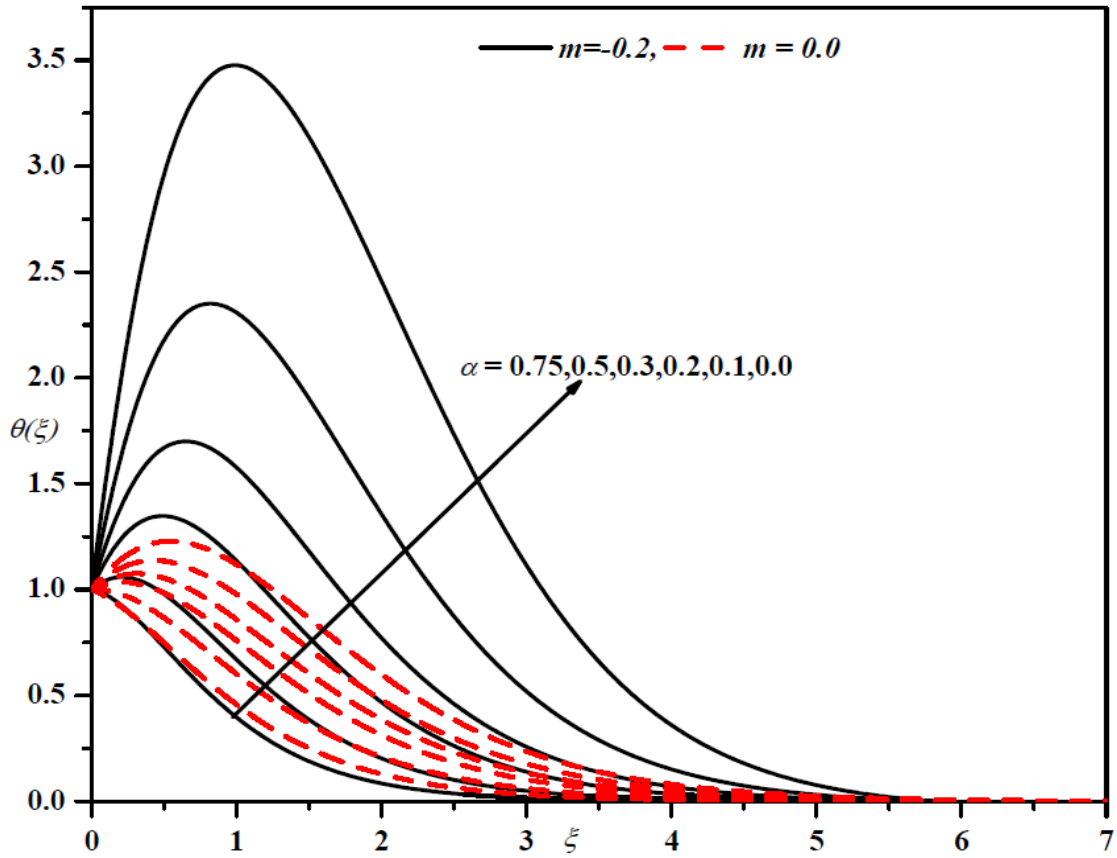

Fig.2(c): Temperature profiles for different values of m and α with $Pr = 1.0,\ \varepsilon = 0.1,\ \lambda = 0.1,\ K_1 = 0.0,\ \theta_r = -5.0$.

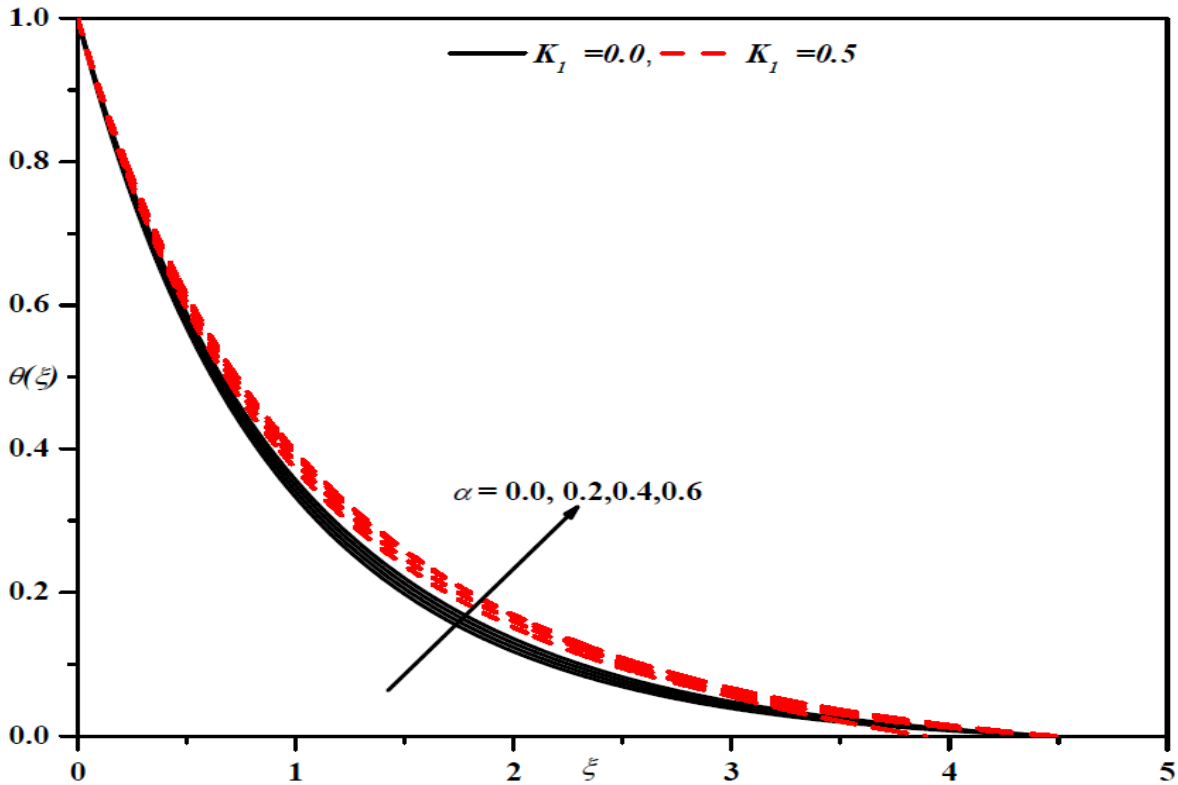

Fig.2(d): Temperature profiles for different values of α and K_1 with $\theta_r = -5.0,\ \lambda = 0.1,\ \varepsilon = 0.1,\ m = 2.0$.

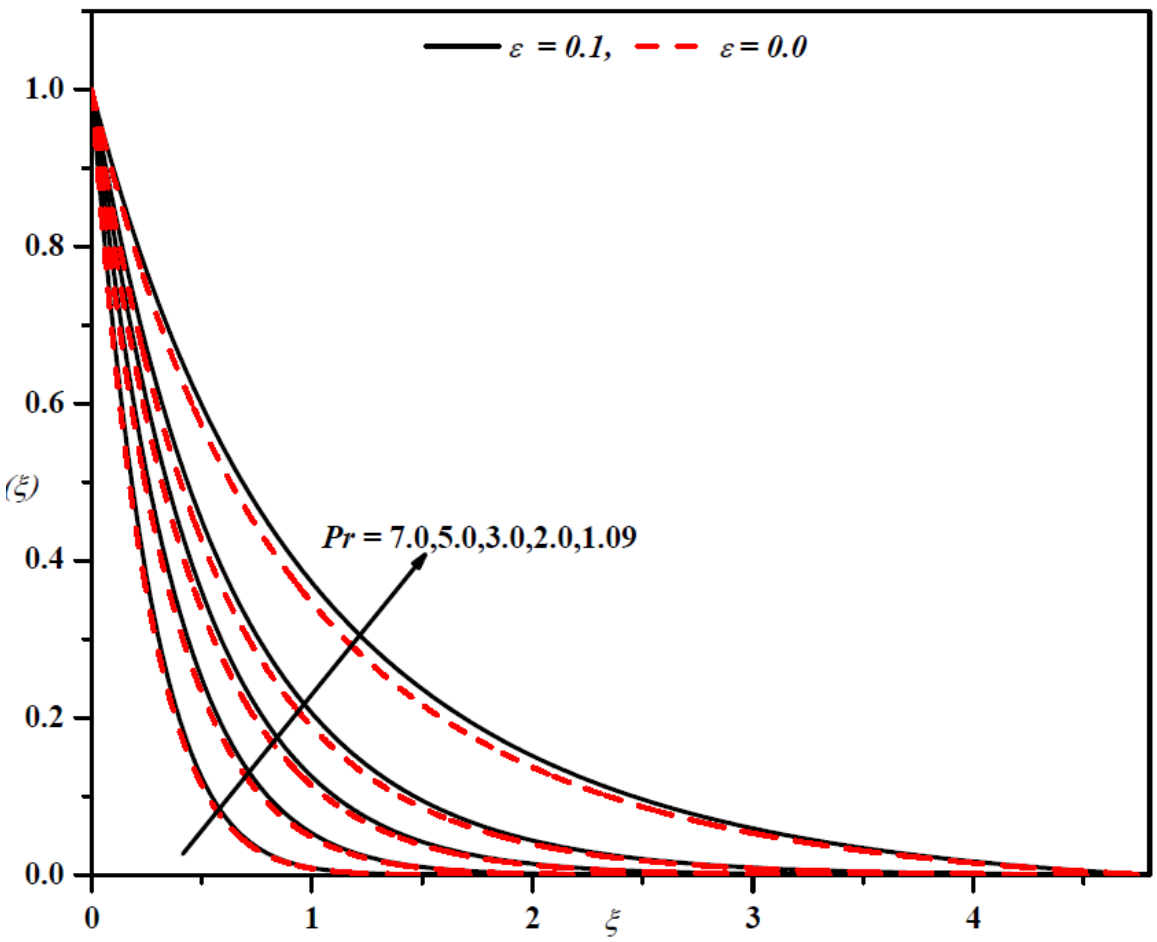

Fig.2(e): Temperature profiles for different values of *Pr* and ε with α =0.5, K_1 = 0.2, θ_r=-5.0, m =2.0, λ = 0.1.

Table I: Comparison of skin friction $-f''(0)$ when for different values of *m* and α with $\theta_r \to \infty,\ m = 0, \varepsilon = 0.0, K_1 = 0.0, \lambda = 0.0.$

α	m	Fang et al. [11]	Khader and Megahed [12]	Present Results
0.5	10	1.0603	1.0603	1.060309
	9	1.0589	1.0588	1.058812
	7	1.0550	1.0551	1.055122
	5	1.0486	1.0486	1.048615
	3	1.0359	1.0358	1.035805
	2	1.0234	1.0234	1.023424
	1	1.0	1.0	1.0
	0.5	0.9799	0.9798	0.979848
	0	0.9576	0.9577	0.957727
	-1/2	1.1667	1.1666	1.166666
0.25	10	1.1433	1.1433	1.143309
	9	1.1404	1.1404	1.140481
	7	1.1323	1.1323	1.132332
	5	1.1186	1.1186	1.118662
	3	1.0905	1.0904	1.090409
	1	1.0	1.0	1.0
	0.5	0.9338	0.9337	0.933770
	0	0.7843	0.7843	0.784309
	-1/3	0.5000	0.5000	0.500000
	-1/2	0.0833	0.08322	0.0832227

Table II: Variation of skin friction $f''(0)$ and wall-temperature gradient $\theta'(0)$ for different values of physical parameters.

m	K_1	θ_r	**Pr**	ε	λ	$\alpha=0.0$		$\alpha=0.1$		$\alpha=0.2$	
						$f''(0)$	$\theta'(0)$	$f''(0)$	$\theta'(0)$	$f''(0)$	$\theta'(0)$
2.0	0.1	-5.0	1.0	0.1	-5.0	-1.545068	-1.080793	-1.522204	-1.068792	-1.499637	-1.057054
					0.0	-1.335278	-1.146790	-1.331519	-1.134678	-1.310604	-1.122755
					0.5	-1.185849	-1.189561	-1.165799	-1.177318	-1.146117	-1.165239
					1.0	-1.031486	-1.222858	-1.012449	-1.210512	-0.993795	-1.198313
5.0	0.5	-5.0	1.0	0.0	0.1	-1.353883	-1.530281	-1.322420	-1.502237	-1.291802	-1.474429
				0.1		-1.352389	-1.380212	-1.320975	-1.356161	-1.290407	-1.332783
				0.2		-1.351008	-1.262758	-1.319643	-1.242086	-1.289123	-1.222008
5.0	0.5	-5.0	1.0	0.1	0.1	-1.353871	-1.383738	-1.320976	-1.135616	-1.290407	-1.332783
			2.0			-1.361864	-2.092309	-1.330033	-2.037640	-1.290407	-1.984734
			5.0			-1.371232	-3.507749	-1.334456	-3.362246	-1.307821	-3.223160
			10.0			-1.376316	-5.101436	-1.344081	-4.806734	-1.312650	-4.529388
λ	K_1	θ_r	Pr	ε	α	$m=-0.2$		$m=0.0$		$m=5.0$	
						$f''(0)$	$\theta'(0)$	$f''(0)$	$\theta'(0)$	$f''(0)$	$\theta'(0)$
0.1	0.0	-5.0	1.0	0.1	0.0	-0.227799	5.478141	-0.631212	0.880672	-1.376995	-1.399540
					0.1	-0.409797	3.568688	-0.718014	0.679241	-1.336629	-1.376940
					0.2	-0.593180	2.335793	-0.808435	0.50008	-1.297614	-1.354864
					0.3	-0.775887	1.545657	-0.902260	0.337709	-1.259952	-1.333293
					0.5	-1.141195	0.598557	-1.099277	0.049424	-1.188558	-1.291576
					0.75	-1.603216	-0.121641	-1.360758	-0.266291	-1.106376	-1.241904
λ	α	m	Pr	ε	θ_r	$\alpha=0.0$		$\alpha=0.5$			
						$f''(0)$	$\theta'(0)$	$f''(0)$	$\theta'(0)$		
0.1	0.0	2.0	1.0	0.1	-10.0	-1.212481	-1.169201	-1.123290	-1.109093		
					-5.0	-1.312789	-1.152769	-1.211471	-1.094139		
					-3.0	-1.435761	-1.132209	-1.317998	-1.075621		
					-2.0	-1.576301	-1.108233	-1.437581	-1.054299		